Comparison of FEM-based 3-D dynamic fracturing simulations using intrinsic and extrinsic cohesive zone models

D. FUKUDA [a]*, E. NIHEI [a], S.H. CHO[b], S.W. OH[b], J. KODAMA[a] and Y. FUJII [a]

[a] *Hokkaido University, Sapporo, Hokkaido, Japan*
[b]*Chonbuk National University, Jeonju, Jeollabuk, Korea*
* d-fukuda@frontier.hokudai.ac.jp (*corresponding author's E-mail)*

Abstract

Smeared crack approach coupled with cohesive zone model has been an attractive way for the realistic simulations of dynamic fracturing of rocks and frequently utilized in the framework of the Finite Element Method (FEM). In many cases, cohesive elements (CEs) with initially-zero-thickness are inserted at the onset of numerical simulations and these are used to express the dynamic fracturing, which is called "intrinsic cohesive zone model (ICZM)". However, since the ICZM must introduce penalty terms to express the intact behavior of the CEs, this tends to render higher compliance of bulk rock, resulting in smaller wave propagation speed. In this paper, by introducing a so-called "extrinsic cohesive zone model (ECZM)", which adaptively inserts the CEs, we compared the results of 3-D dynamic fracturing simulations by the ICZM and ECZM using the experimental data obtained from the dynamic spalling test for rocks. Using the same Young's modulus, Poisson's ratio, density and strengths estimated from the experiments, our results suggest that the outcome of the ICZM and experiment showed large discrepancy especially for the intact stress wave propagation while the ECZM showed good agreement with the experiment. Therefore, our results could have some implications on the current situation in which more and more simulations using the ICZM such as in hybrid FEM-DEM have been applied to rock fracture mechanics problems.

Keywords: Dynamic fracture, Rocks, Cohesive zone model, 3D DFPA, 3D hybrid FEM-DEM

1. Introduction

Hybrid finite element method (FEM)-discrete element method (DEM) has been increasingly applied to the simulation of dynamic fracturing of rocks including blasting problems. In the majority of these simulations in previous research, cohesive zone models have been applied where cohesive elements (CEs) with initially-zero-thickness were inserted at the onset of simulation (e.g. Mahabadi et al., 2010; Rougier et al., 2014; An et al., 2017) and used to express fracturing behavior. This approach is a so-called "intrinsic cohesive zone model (ICZM)". Since the ICZM must introduce penalty terms to express the intact behavior of the CEs, this may render higher compliance of bulk rock, resulting in smaller wave propagation speed. On the other hand, a so-called "extrinsic cohesive zone model (ECZM)" has also been proposed for ceramics and concrete which adaptively inserts the CEs where and when they are needed (e.g. Ortiz and Pandolfi, 1999; Ruiz et al, 2001; Pandolfi and Ortiz, 2002). This approach has been rarely applied to the dynamic fracturing problems of rocks except our in-house 2-D Dynamic Fracture Process Analysis (DFPA) code (e.g. Cho et al., 2003). In addition, it seems that comparative work of the results based on the ICZM and ECZM has not been found in the rock mechanics discipline.

In this paper, by incorporating both the ICZM and ECZM into our in-house 3-D DFPA code which has been recently developed by fortran (e.g. Fukuda et al. 2016), we compared the results of 3-D fracturing simulations of dynamic spalling test for a rock based on the ICZM and ECZM, respectively. Then, we discuss the advantage of the ECZM and indicate some caution on the use of the ICZM for the simulation of dynamic fracture of rocks.

2. Dynamic fracturing simulation based on 3-D DFPA code using ICZ and ECZM

The behavior of intact rock before the onset of micro-fracturing is assumed to be that of an isotropic elastic solid with viscous damping and is modeled by an assembly of continuum solid elements, i.e., 4-node tetrahedral finite elements (TET4s), for the spatial discretization of FEM.

The fracturing process of rock, i.e. the opening and sliding of micro-cracks, is modelled through a cohesive zone model. Tensile and shear softening curves are used, which are expressed as a function of crack opening and sliding to reflect the behavior of the fracture process zone in front of the crack tips. These are expressed by 6-node initially zero-thickness cohesive elements (CEs) (see Fig. 1(a)). For the insertion of the CEs, two possibilities are considered. The first is to insert the CEs into all the boundaries of the TET4s corresponding to rock at the beginning of the analysis, i.e. the ICZM. The second approach is to dynamically, or adaptively, insert the CEs into the particular boundaries of the TET4s with the help of adaptive remeshing under a given failure criterion, i.e. the ECZM. As shown in Fig.1(b), the apparent intact behavior of the CEs must be specified in the ICZM, which requires the introduction of penalty parameters, a.k.a. stiffness of the CEs before the onset of softening, and the time step increment must be carefully chosen to be relatively smaller. In this respect, the ECZM is better as shown in Fig.1(c) as no penalty parameters before the onset of fracturing are required. This is because the intact elastic behavior is expressed by TET4s in the ECZM. Note that, due to page limitation, only Mode I behavior based on tensile softening is illustrated in Fig.1(b)(c) while Mode II behavior has also been implemented in our code based on slip weakening which is characterized by Mode II fracture energy, G_{fII}, and shear strength modeled by Mohr-Coulomb model. To consider heterogeneity of rocks, the tensile strength and cohesion were spatially distributed based on the Weibull's strength distribution (e.g. Cho et al. 2003).

When either critical values of critical crack opening or slip are achieved in a CE, the CE is deactivated and its surfaces are considered as macro fracture surfaces. After this, the contact processes between the newly created macro fracture surfaces are modelled by the penalty method. (See. Munjiza et al. (2011) for further detail.).

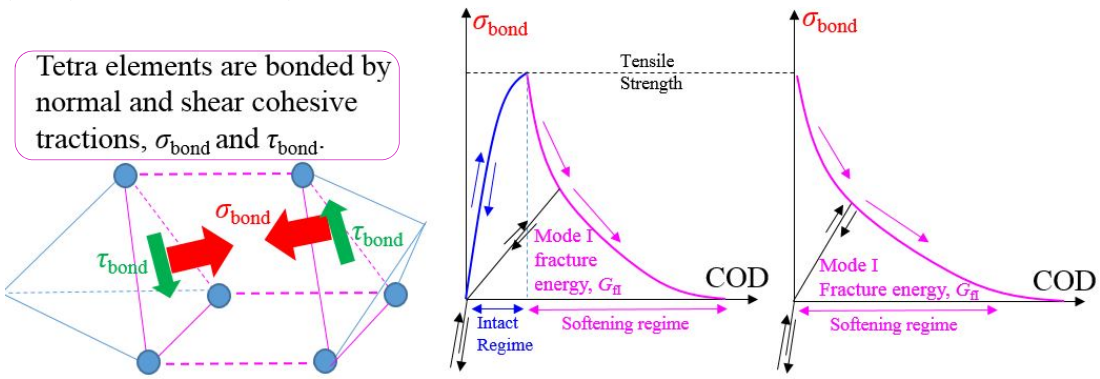

(a) (b) (c)

Fig. 1. Schematic illustration of (a) CE and its constitutive behavior (Mode I) for (b) ICZM and (c)ECZM.

3. 3-D DFPA for dynamic spalling test (dynamic tension test)

This paper compares results of the DFPAs for the dynamic spalling test of Geochang granite based on Hopkinson pressure bar apparatus (See. Fig.2(a)) using both the ICZM and ECZM. In this test, a striker bar is impacted onto one end of an incident bar (IB) with the help of gas pressure. The approximately 1-D compressive stress wave propagates toward the other end of the IB where the cylindrical rock specimen is attached. When the stress wave arrives at the interface between the IB and rock specimen, some portion of the compressive stress is reflected back to the IB as a tensile stress wave while the remaining portion is transmitted into the rock specimen as a compressive stress wave. The magnitude of this compressive stress wave is adjusted in a way that no fracturing due to the compression occurs. When this compressive stress wave arrives at the free end of the rock specimen, the sign of the stress wave is reversed and a tensile stress wave is propagated back to the IB. This causes tensile fracturing at some distance away from the free end of the rock, a.k.a. spalling. During this test, the location of initially formed macro spall fracture plane is observed by a high-speed camera and the free surface particle velocity (FSPV) of the free end of the rock is measured by laser. Both of these are used for the determination of dynamic tensile strength of the target rock. Thus, in case detailed investigation is necessary for this test, the numerical simulation must predict both the location of the fracture plane and the time history of the measured FSPV well.

For this purpose, we prepared the 3-D numerical rock model as shown in Fig.2(b) which has the same size as that in the experiment. For simplicity, the stress wave profile measured in the IB was converted to the pressure time history, $P(t)$, by assuming that the impact between the IB and the rock specimen is elastic, and this $P(t)$ was applied to one end of the numerical rock model. Using measured

rock density (2641.0 kg/m^3), P- and S-wave velocities of rock, we computed dynamic Young's modulus, E_{rock} (=40.6 GPa), and dynamic Poisson's ratio, ν_{rock} (=0.2 GPa) for the DFPA. By conducting preliminary analyses, we decided to set the average tensile strength = 15 MPa which is 1.5 times larger than that of static Brazilian test and Mode I fracture energy G_{fI} = 400 J/m^2. Although the Mode II fracturing can also be simulated in the DFPA, we found that the simulation results are less sensitive to the Mode II-related mechanical properties. Thus, we just used internal friction angle = 50 degrees, average cohesion = 36.7 MPa and G_{fII} = 400 J/m^2. The coefficient of uniformity, m, was set to be 5 based on Cho et al. (2003). For the case of the ICZM, all the penalty factors for contact, crack closing, crack opening and crack slip was set to be E_{rock} since the DFPA code utilized an explicit time integration scheme and the simulations can be finished within reasonable time with these penalty values. For the case of the ECZM, penalty factors for contact and crack closing were set to be E_{rock} where penalty factors for crack opening and slip are not needed. With these input parameter settings, we compare the behavior of the ICZM and ECZM using same elastic constants and strengths.

4. Results and discussion

In Fig. 3(a), comparison of FSPV time history obtained from both the experiment and DFPAs are shown. In the figure, the results of the ECZM and ICZM (Case 1) were obtained using the aforementioned input parameters. The ECZM captured the FSPV time history quite well while the ICZM (Case 1) and the experiment showed significant discrepancy not only for the arrival of stress wave but also for the peak value of the FSPV, which are quite important parameters in this test (See. Cho et al. (2003) for further detail.). This is due to the introduction of the penalty factors for crack opening and slip, which increase the compliance of the bulk rock model. To validate this, we additionally conducted the DFPA with the ICZM in which dynamic Young's modulus and penalty factors for crack closing, crack opening and crack slip was increased to $3E_{rock}$. Ideally, we should have increased the penalty factors only and not the dynamic Young's modulus. However, increasing only the penalty factors makes the stable time step size unrealistically smaller. The corresponding results are shown by "ICZM (Case 2)" in Fig.3. It is evident from the figure that the ICZM (Case 2) showed better agreement with the experiment.

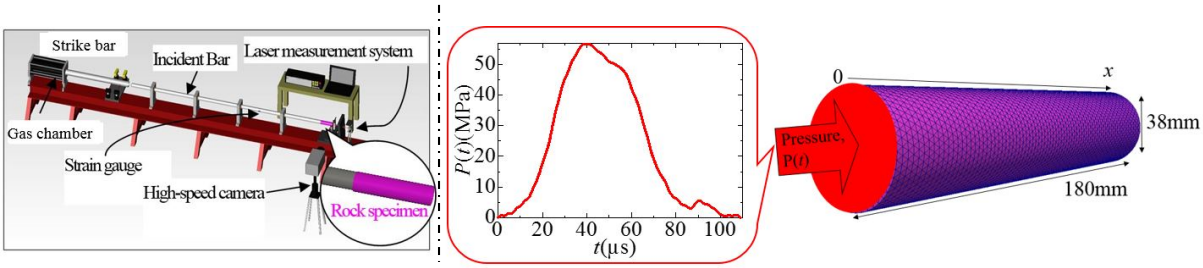

(a) (b)

Fig. 2. (a)Schematic illustration of spalling test and (b)corresponding numerical rock model used in 3D DFPA.

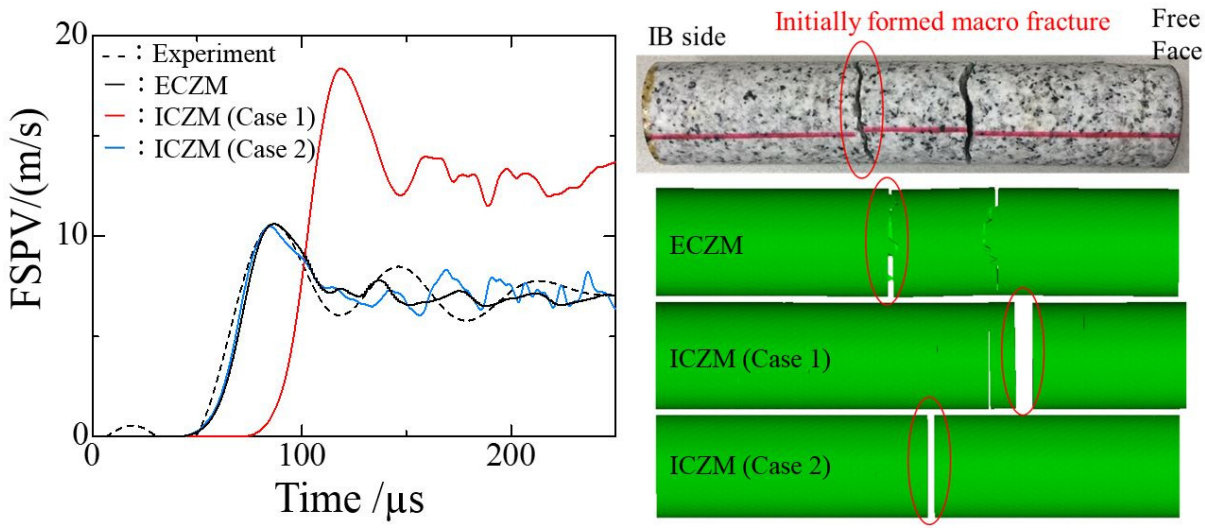

(a) FSPV (b)Fracture pattern

Fig. 3. Comparison of experimental and DFPA results.

In Fig. 3(b), comparison of macro spall fracture planes obtained from both the experiment and DFPA are shown. Again, owing to the large compliance in the ICZM (Case 1), the location of macro spall fracture planes is largely different from the experiment. Meanwhile, the ECZM captured the spall fracture locations much better. When the penalty factors and dynamic Young's modulus were increased in the ICZM (Case 2), the location of main macro spall fracture plane became closer to the experiment than the ICZM (Case 1).

From above comparisons, we can conclude that the approach using the ECZM can simulate, at least, the dynamic spalling test of rock better than that using the ICZM. Considering the result of ICZM (Case 2) and quite realistic simulation results of the dynamic Brazilian test using the ICZM in previous research (e.g. Mahabadi et al., 2010; Rougier et al., 2014), it can still be a powerful approach as long as the proper calibration is conducted in which penalty parameters and elastic constants are properly adjusted to make the apparent stress wave propagation speed closer to the experiments. Since the spalling test uses much longer sample size than the dynamic Brazilian disc, the aforementioned non-negligible discrepancy between the simulation and experiment seems to be obtained. In this respect, since the ECZM is just a pure FEM when the CEs do not exist, intact stress wave propagation is well captured by just measuring the density and wave speeds of the target rock sample.

However, one of the advantages of the ICZM is in that its implementation and application of parallel computing is straightforward as in Rougier et al. (2014) and Fukuda et al. (2016), and less computer memory is required. On the other hand, the ECZM tends to require an elaborate adaptive remeshing technique as in Pandolfi and Ortiz (2002) and Cho et al. (2003), which tends to require a larger amount of computer memory for storing the geometrical data. In addition, when the number of pre-existing fractures is very large, the ICZM approach can be more attractive than the ECZM. Therefore, the choice of either ICZM or ECZM should depend on the problem of interest.

5. Conclusion

This paper compared the results of 3-D dynamic fracturing simulations by the ICZM and ECZM, respectively, using the experimental data obtained from the dynamic spalling test for rocks. It is suggested that the ICZM using the same mechanical properties as the ECZM shows large discrepancy from the experiment for the intact stress wave propagation while the ECZM shows quite good agreement with the experiments although the ICZM could still be used with careful calibration of input parameters. Considering the current situation in which more and more hybrid FEM-DEM simulations with the cohesive zone model have been applied to important rock dynamics problems, we suggest that the hybrid FEM-DEM with the ICZM should be used with extra caution for the simulations where not only the fracturing process but also the intact stress wave propagation is important.

References

An, H.M., Liu, H.Y., Han, H., Zheng, X., Wang, X.G., Hybrid finite-discrete element modelling of dynamic fracture and resultant fragment casting and muck-piling by rock blast, Computers and Geotechnics 81(2017), 322-345.

Cho, S.H., Ogata, Y., Katsuhiko K., Strain rate dependency of the dynamic tensile strength of rock. Int J Rock Mech Min Sci 40 (2003), 763–777.

Fukuda, D., Cho, S.H., Oh, S.W., Kodama J., Fujii, Y., Development and validation of GPU-based 3D-dynamic fracturing process analysis code for rocks subjected to impact loading, 22nd DYMAT Technical Meeting, Grenoble, France, Oct., 2016, paper ID 95439.

Mahabadi, O.K., Cottrell, B.E., Grasselli, G., An Example of Realistic Modelling of Rock Dynamics Problems: FEM/DEM Simulation of Dynamic Brazilian Test on Barre Granite, Rock Mech Rock Eng 43(2010), 707–716.

Munjiza, A., Knight, E., Rougier, E., Computational Mechanics of Discontinua, John Wiley & Sons, Ltd, Chichester, UK, 2011.

Ortiz, M., Pandolfi, A., Finite-deformation irreversible cohesive elements for three dimensional crack-propagation analysis. Int J Num Meth Eng 44(1999),1267–1282.

Pandolfi, A., Ortiz, M., An efficient adaptive procedure for three-dimensional fragmentation simulations. Eng Comput 18(2002),148–159.

Rougier, E., Knight, E.E., Broome, S.T., Sussman, A.J., Munjiza, A., Validation of a three-dimensional Finite-Discrete Element Method using experimental results of the Split Hopkinson Pressure Bar test, Int J Rock Mech Min Sci 70(2014), 101–108.

Ruiz, G., Ortiz, M., Pandolfi, A., Three-dimensional finite-element simulation of the dynamic Brazilian tests on concrete cylinders, Int J Numer Meth Eng 48(2000), 963–994.